frontiers in Environmental Science

ORIGINAL RESEARCH
published: 25 September 2018
doi: 10.3389/fenvs.2018.00101

pH as a Primary Control in Environmental Microbiology: 2. Kinetic Perspective

Qusheng Jin[1]* *and Matthew F. Kirk*[2]

[1] Department of Earth Sciences, University of Oregon, Eugene, OR, United States, [2] Department of Geology, Kansas State University, Manhattan, KS, United States

In a companion paper, we examined the thermodynamic responses of microbial redox reactions to pH changes. Here we explore how these thermodynamic responses may affect the composition and function of microbial communities. We simulate butyrate syntrophic oxidation, sulfate reduction, and methanogenesis by microbial consortia at pH ranging from 7 to 5. The simulation accounts for the thermodynamics of microbial metabolisms and the interactions among microbes. The results show that thermodynamic responses to variation in pH can be strong enough to speed up or slow down microbial metabolisms. These kinetic changes then shape the outcome of microbial interactions, including the membership and activity of microbial consortia. Moreover, the kinetic changes modulate carbon fluxes and the efficiency of methane production. The simulation results support the hypothesis that environmental pH can shape the composition and metabolic function of microbial communities by changing the energy yields of redox reactions. They also add to the current theories of microbial ecology. Specifically, due to pH-induced thermodynamic responses, the principle of competitive exclusion fails for microbial processes with significant thermodynamic limitations, which allows the co-occurrence of competing respiration reactions in natural environments. Taken together, these results confirm that pH is a primary control in environmental microbiology. They also highlight the feasibility and potential of biogeochemical kinetic modeling in uncovering and illuminating mechanistic relationships between environmental parameters and microbial communities.

Keywords: bioenergetics, butyrate oxidation, sulfate reduction, methanogenesis, microbial kinetics

OPEN ACCESS

Edited by:
Alain F. Plante,
University of Pennsylvania,
United States

Reviewed by:
John W. Moreau,
The University of Melbourne, Australia
Juan M. Gonzalez,
Consejo Superior de Investigaciones Científicas (CSIC), Spain

***Correspondence:**
Qusheng Jin
qjin@uoregon.edu

Specialty section:
This article was submitted to Microbiological Chemistry and Geomicrobiology, a section of the journal Frontiers in Environmental Science

Received: *21 March 2018*
Accepted: *23 August 2018*
Published: *25 September 2018*

Citation:
Jin Q and Kirk MF (2018) pH as a Primary Control in Environmental Microbiology: 2. Kinetic Perspective. Front. Environ. Sci. 6:101. doi: 10.3389/fenvs.2018.00101

INTRODUCTION

Environmental pH is one of the most informative parameters for studying microbes in natural environments. pH represents the chemical activities of protons—a reactant that participates in biological energy conservation, interacts with cellular surface components and structures, and involves in metabolism-related chemical reactions, including redox reactions, mineral dissolution and precipitation, and reactions of natural organic matter (Kinniburgh et al., 1999; Konings et al., 2002; Paul et al., 2006). Reflecting these relationships, pH correlates with community composition across a wide range of biogeochemical conditions (Thompson et al., 2017), and pH variation induces significant changes in the metabolic functions of microbial communities (Kotsyurbenko et al., 2004; Ye et al., 2012).

In a companion paper (Jin and Kirk, 2018), we hypothesize that the correlation between pH and microbial communities may also reflect the thermodynamic and kinetic responses of microbial metabolisms to pH variation. This hypothesis is based on the dependence of chemotrophic microbes on chemical energy in the environment (Thauer et al., 1977; Jin, 2012). Chemotrophs liberate chemical energy in the environment by catalyzing redox reactions and save a part of the liberated energy by making adenosine triphosphate (ATP) molecules. They then spend the ATPs to maintain biomass and make new cells. Any factors that influence the energy available in the environment, therefore, have the potential to affect the metabolisms of individual microbial groups and the composition and metabolic activity of microbial communities.

To test this hypothesis, we examined the effect of pH variation on the energy yields of microbial redox reactions (Jin and Kirk, 2018). We focused on redox reactions involved in organic matter degradation, including syntrophic oxidation, iron reduction, sulfate reduction, and methanogenesis, and computed their energy yields at pH ranging from 1 to 14. The results show that energy yields vary significantly in response to both direct and indirect impacts of pH variation. The direct impact is due to the changes in proton chemical activities and applies to the reactions that consume or produce protons; the indirect impact comes from the control of pH on chemical speciation–pH variation affects the distribution of solute mass among possible chemical species and thus the activities of chemical species involved in microbial reactions.

These results demonstrate that pH variations can alter the energy yields of microbial redox reactions. However, thermodynamics alone is limited in its ability to predict the metabolic rates and population sizes of microbes or to account for the correlation between pH and microbial communities (Bethke et al., 2011; Amenabar et al., 2017). These limitations arise in part from the complexity of microbial metabolisms in natural settings. In addition to thermodynamics, microbial metabolisms are subject to control by a wide range of biogeochemical factors, including substrate availability, geochemical reactions, and microbial interactions (Panikov, 1995; Jin et al., 2013). But most thermodynamic calculations are reaction specific, and do not explicitly consider concurrent geochemical reactions or microbial metabolisms.

Here we apply kinetic modeling to explore how pH may influence the composition and metabolic activity of simple microbial consortia. According to microbial kinetic theory, the rates of microbial metabolisms depend on the thermodynamic drives of microbial respiration, the differences between the energy available in the environment and the energy conserved by ATP synthesis (Jin and Bethke, 2003, 2007). A change in pH could raise or lower the thermodynamic drives and speed up or slow down individual microbial metabolisms, which in turn shape microbial interactions and the membership of microbial consortia.

We simulate microbial metabolisms using biogeochemical reaction modeling (Bethke, 2008; Jin et al., 2013). In addition to changing the energy yields of redox reactions, pH also directly affects the kinetic parameters of microbes. In our simulation, we assume that pH only impacts the energy yields. This assumption is of course an oversimplification but it allows us to concentrate on the outcome of pH-induced changes of energy yields. We can include the changes of microbial kinetic parameters, but the results would bear the combined effects of microbial kinetic and thermodynamic responses. Thus, they would not be straightforward in illustrating the significance of the thermodynamic effect—the focus of the current study.

We focus on syntrophic butyrate oxidation, sulfate reduction, and methanogenesis. Butyrate is a common intermediate in the degradation of natural organic matter whereas sulfate reduction and methanogenesis are common microbial processes in anoxic environments (Monokova, 1975; Molongoski and Klug, 1980; Lovley and Klug, 1982). Our simulation considers microbial interactions, including competition and syntrophy, and computes rates of respiration and growth by accounting for the chemical energy in the environment. We seek to demonstrate how pH can influence the outcome of microbial interactions—the membership and activity of microbial consortia—by changing the energy yields of redox reactions.

METHODS

We simulate the progress of microbial metabolisms using the rates of microbial respiration, biosynthesis, and maintenance. Microbial respiration couples redox reactions to the synthesis of ATP. The redox reactions can be represented as

$$\sum_{\mathrm{D}} \nu_{\mathrm{D}} \mathrm{D} + \sum_{\mathrm{A}} \nu_{\mathrm{A}} \mathrm{A} \rightleftarrows \sum_{\mathrm{D}^+} \nu_{\mathrm{D}^+} \mathrm{D}^+ + \sum_{\mathrm{A}^-} \nu_{\mathrm{A}^-} \mathrm{A}^-, \qquad (1)$$

where D and D^+ are electron donors and their oxidized forms, respectively, A and A^- are electron acceptors and their reduced forms, respectively, and ν_D and others are stoichiometric coefficients. The energies ΔG_A available from the reactions are the negative of the Gibbs free energy changes [J·(mol reaction)$^{-1}$, or J·mol^{-1}], and are calculated according to

$$\Delta G_A = -\Delta G^o - RT \ln \left(\frac{\prod_{\mathrm{D}^+} \mathrm{a}_{\mathrm{D}^+}^{\nu_{\mathrm{D}^+}} \cdot \prod_{\mathrm{A}^-} \mathrm{a}_{\mathrm{A}^-}^{\nu_{\mathrm{A}^-}}}{\prod_{\mathrm{D}} \mathrm{a}_{\mathrm{D}}^{\nu_{\mathrm{D}}} \cdot \prod_{\mathrm{A}} \mathrm{a}_{\mathrm{A}}^{\nu_{\mathrm{A}}}} \right), \qquad (2)$$

where ΔG° is the standard Gibbs free energy change, a is the chemical activity, R is the gas constant (J·mol^{-1}·K^{-1}), and T is the temperature in kelvin (K). Chemical activity is calculated as the product of activity coefficients (M^{-1}) and molal concentrations of chemical species. Activity coefficients are calculated according to an extended form of the Debye-Hückel equation (Helgeson, 1969).

Respiration rate r (mol·kg^{-1}·s^{-1}, mol per kg water per s) can be calculated according to the thermodynamically consistent rate law (Jin and Bethke, 2005, 2007):

$$r = k \cdot [X] \cdot \prod_i F_i, \qquad (3)$$

where k is the rate constant [mol·(g dry weight)$^{-1}$·s^{-1}, or mol·g^{-1}·s^{-1}], [X] is the biomass concentration [g dry weight·(kg

water)$^{-1}$, or g·kg^{-1}], and F_i represents different controlling factors, including the kinetic factors of electron donor (F_D) and acceptor (F_A), and the thermodynamic potential factor (F_T). The kinetic factors are calculated according to

$$F_D = \frac{m_D}{K_D + m_D} \tag{4}$$

and

$$F_A = \frac{m_A}{K_A + m_A}, \tag{5}$$

where m_D and m_A are the molal concentrations of electron donor and acceptor, respectively, and K_D and K_A are the half-saturation constants (M) for electron donor and acceptor, respectively. The thermodynamic potential factor is calculated according to

$$F_T = 1 - \exp\left(-\frac{f}{\chi \cdot RT}\right), \tag{6}$$

where f is the thermodynamic drive (J·mol^{-1}), and χ is the average stoichiometric number. The thermodynamic drive,

$$f = \Delta G_A - \Delta G_C, \tag{7}$$

is the difference between the energy ΔG_A (J·mol^{-1}) available in the environment and the energy ΔG_C (J·mol^{-1}) conserved by respiration.

According to Jin (2007), the energy ΔG_C (J·mol^{-1}) conserved by syntrophic butyrate oxidizers is a function of hydrogen partial pressure P_{H_2} (atm),

$$\Delta G_C = \begin{cases} 3.5 \times 10^4, & P_{H_2} < 10^{-9}\text{atm} \\ -1.78 \times 10^4 - 2.5 \times 10^3 \cdot \ln\left(P_{H_2}\right), & 10^{-9}\text{atm} < P_{H_2} < 10^{-3}\text{atm} \\ 0, & P_{H_2} > 10^{-3}\text{atm} \end{cases}. \tag{8}$$

According to this model, the conserved energy reaches its largest value at H_2 partial pressure less than 10^{-9} atm, and declines with increasing H_2 partial pressure. At the partial pressure of 10^{-3} atm or more, the conserved energy declines to 0.

For sulfate reducers and methanogens, the conserved energy ΔG_C is calculated as

$$\Delta G_C = \nu_P \cdot \Delta G_P, \tag{9}$$

the product of the ATP yield ν_P of respiration and the phosphorylation energy ΔG_P (Jin and Bethke, 2002, 2003). The phosphorylation energy is the energy required to synthesize ATP from ADP and phosphate in the cytoplasm, and its value is taken as 45 kJ·(mol ATP)$^{-1}$ (Jin, 2012).

Microbes utilize the conserved energy ΔG_C to synthesize biomass. The rate at which the biomass concentration [X] changes with time, or the net growth rate, is

$$\frac{d[X]}{dt} = Y \cdot r - D \cdot [X], \tag{10}$$

where Y is the biomass yield, the grams of biomass dry weight synthesized per mol reaction (g·mol^{-1}), and D is the specific rate of maintenance and death (s^{-1}) (van Bodegom, 2007). The product of the growth yield and respiration rate, $Y \cdot r$, gives the biosynthesis rate. Equation (10) neglects that many microbes can persist through adverse environmental conditions via dormancy and other survival mechanisms. Instead, it assumes that microbial population sizes depend solely on biosynthesis rate relative to the rate of maintenance.

We simulate the metabolisms of neutrophilic syntrophic butyrate oxidizers, sulfate reducers, and methanogens using the React program of the software package Geochemist's Workbench version 9.0 (Bethke, 2008). The simulation assumes that aqueous chemical speciation is at thermodynamic equilibrium, and describes these reactions on the basis of the updated LLNL Thermodynamic Database (Delany and Lundeen, 1990). Evaluating microbial rate laws (Equations 3 and 10) requires a series of microbial parameters; their values are listed in **Table 1**.

We carry out the simulation by varying pH from 7 to 5. Most neutrophilic microbes live over 4 pH units (Rosso et al., 1995). Taking pH 7 as the optimal growth pH, a decrease of 2 pH units would decrease microbial growth rates to 0. Hence we simulate the metabolisms at pH ranging from 7 to 5. We assume that microbial parameters, such as rate constant k and half-saturation constants K_D and K_A, remain constant at different pHs. This assumption is necessary for testing the hypothesis that microbial thermodynamic responses to pH are strong enough to modulate the kinetics of microbial metabolisms and the outcome of microbial interactions. The input scripts are available in **Supplementary Material**.

RESULTS

In the companion paper (Jin and Kirk, 2018), we analyzed the thermodynamic responses of individual redox reactions to pH changes. Microbes rarely, if ever, live in isolation in nature. Instead, they often join each other in communities to carry out a network of biogeochemical reactions and perform a wide range of ecological functions (Nielsen et al., 2011; Xavier, 2011). By working together, microbes build different working relationships, such as competition and syntrophy. Here we apply biogeochemical reaction modeling to predict how the thermodynamic responses to pH may influence the outcome of microbial competition and syntrophy.

Competition

A classic example of microbial competition is the competition for acetate between sulfate reducers and methanogens (Lovley and Philips, 1987). Sulfate reducers oxidize acetate to inorganic carbon by reducing sulfate to sulfide,

$$\text{Acetate} + SO_4^{2-} + H^+ \rightleftarrows 2HCO_3^- + H_2S. \tag{11}$$

Methanogens convert acetate to CO_2 and methane,

$$\text{Acetate} + H_2O \rightleftarrows HCO_3^- + CH_4. \tag{12}$$

In the companion paper (Jin and Kirk, 2018), we show that a pH decrease from 7 to 5 raises the energy yields of both

TABLE 1 | Kinetic parameters (rate constant k, and half-saturation constant K_D and K_A), growth parameters (growth yield Y and specific maintenance rate D), and thermodynamic parameters (ATP yield ν_P and average stoichiometric number χ) of microbial metabolism.

Microbe	Reaction[a]	Kinetic parameter[b]			Growth parameter		Thermodynamic parameter[c]	
		k (mol·g^{-1}·s^{-1})	K_D (molal)	K_A (molal)[c]	Y[d] (g·mol^{-1})	D[e] (s^{-1})	ν_P	χ
Strain IB	Butyrate oxidation (Equation 13)	2.0×10^{-6}	6.5×10^{-5}		–[f]	10^{-7}	–[g]	2
D. postgatei	Sulfate reduction (Equation 11)	1.0×10^{-6}	2.3×10^{-4}	1.5×10^{-4}	5.0	10^{-7}	1.0	6
M. barkeri	Acetoclastic methanogenesis (Equation 12)	1.0×10^{-6}	3.0×10^{-3}		2.1	10^{-7}	0.5	2
M. mazei	Acetoclastic methanogenesis (Equation 12)	2.0×10^{-6}	2.0×10^{-3}		3.1	10^{-7}	0.74	2
M. formicium	Hydrogenotrophic methanogenesis (Equation 14)	2.0×10^{-6}	1.0×10^{-7}		2.5	10^{-7}	0.5	2

[a]*Numbers in parentheses are equation numbers in text.* [b]*Jin and Roden (2011) and Jin and Kirk (2016).* [c]*Only consider the kinetic factor of sulfate.* [d]*Jin (2012).* [e]*Jin and Roden (2011).* [f]*The yield is computed according to* $Y = Y_G \cdot \Delta G_C$*, where* Y_G *is the biomass yield per unit energy conserved, and the value is 0.1 g·kJ*$^{-1}$ *(Jin, 2007).* [g]*See text.*

reactions and thus has the potential to speed up the metabolisms of both microbial groups. Nevertheless, according to the principle of competitive exclusion, sulfate reducers win the competition against methanogens because sulfate reducers can hold acetate concentrations either below the thresholds required by running methanogenesis (Lovley et al., 1982) or below the levels required for sustaining methanogen populations (Bethke et al., 2008).

Closed Environment

We first simulate the competition between a sulfate reducer and a methanogen in a closed environment. Schönheit et al. (1982) monitored acetate oxidation in laboratory batch reactors by a representative sulfate reducer—*Desulfobacter postgatei*—and by a model methanogen—*Methanosarcina barkeri*. In their experiments, the two microbes grew together at 30°C in growth media with pH 6.9, 10 mmolal acetate, and 20 mmolal sulfate. We simulated the experiments by taking the initial biomass concentrations at 1.5 g·(kg H_2O)$^{-1}$ for *D. postgatei* and 2.0 g·(kg H_2O)$^{-1}$ for *M. barkeri*. These initial biomass concentrations are estimated by fitting the simulation results to the concentrations of acetate, methane, and sulfide during the first hour of the experiments (**Figure 1**). Also, to best fit the experimental observations, we set a lag time of 10 min before the two microbes start to consume acetate.

Figure 1 shows how chemical concentrations change with time according to the experimental observations and the simulation results. Acetate concentration decreases with time while sulfide and methane concentrations increase. After 1.5 h, methane concentration reaches a constant value. An hour later, sulfide also stabilizes. The simulation results predict that neither microbe grows much—during the experiments, their biomass concentrations increase by less than 2% of the initial concentrations (results not shown). But the rates of sulfate reduction and methanogenesis vary significantly over time (**Figure 2**). Both rates are about 1.5×10^{-6} molal·s^{-1} at the beginning of the experiments and decrease almost linearly with time. The rates of methanogenesis and sulfate reduction fall near 0 around hour 1.7 and 3, respectively. In other words, methanogenesis stops earlier than sulfate reduction. The modeling results also show that *D. postgatei* and *M. barkeri* differ from each other in the contribution to acetate consumption. Overall, 59% of the acetate is consumed by *D. postgatei* while *M. barkeri* uses the remaining 41%.

The simulation results demonstrate that the energy availability limits the progress of both sulfate reduction and methanogenesis (**Figure 3**). At the beginning of the experiments, the energy available to *D. postgatei* is 75 kJ·mol^{-1}, much larger than that to *M. barkeri*, 40 kJ·mol^{-1}. As the experiments progress, the acetate consumption and the accumulation of sulfide, bicarbonate, and methane decrease the available energy (**Figures 1**, **3A,B**). About 1.5 h into the experiments, energy available to *M. barkeri* decreases to 25 kJmol^{-1} and the thermodynamic drive disappears. As such, the thermodynamic potential factor decreases to zero and methanogenesis ceases (Equation 3). At this time, energy available to *D. postgatei* is 55 kJmol^{-1}, still larger than the energy it conserves, allowing sulfate reduction to continue. After 2 h into the experiment, however, energy available to *D. postgatei* approaches 45 kJmol^{-1}, the energy conserved by the organism, and the reaction slows. This result supports the hypothesis that sulfate reducers can win the competition by lowering acetate below the threshold level required for running methanogenesis (Lovley et al., 1982).

Figures 1, **2** also show the simulation results at pH 6 and 5. According to these results, sulfide production is faster at lower pH. For example, at the beginning of the experiments, sulfide is produced at 1.08×10^{-6}, 1.22×10^{-6}, and 1.35×10^{-6} molal·s^{-1} at pH 7, 6, and 5, respectively. Accordingly, sulfide reaches its maximum concentration after 2.5, 2, and 1.7 h, respectively. In comparison, the pH changes have little impact on methane production. Methane is produced $1.38 \pm 0.05 \times 10^{-6}$ molal·s^{-1} in each simulation.

Figure 3A shows that the energy yield of *D. postgatei* responds significantly to pH changes. The pH decreases from 7 to 6 and from 6 to 5 raise the energy yield by about 7.1 kJ·mol^{-1} and 13.6 kJ·mol^{-1}, respectively. As a result, the thermodynamic potential factor increases, speeding up sulfate reduction (**Figures 2A**, **3C**).

Figure 3B shows that the energy yield of methanogenesis also responds to the pH changes. The pH decreases from 7 to 6 and from 6 to 5 raise the energy yield by about 1.4 kJ·mol^{-1} and 3.6 kJ·mol^{-1}, respectively. These increases raise the thermodynamic potential factor (**Figure 3D**). However, the rate does not respond notably to the pH changes because, in

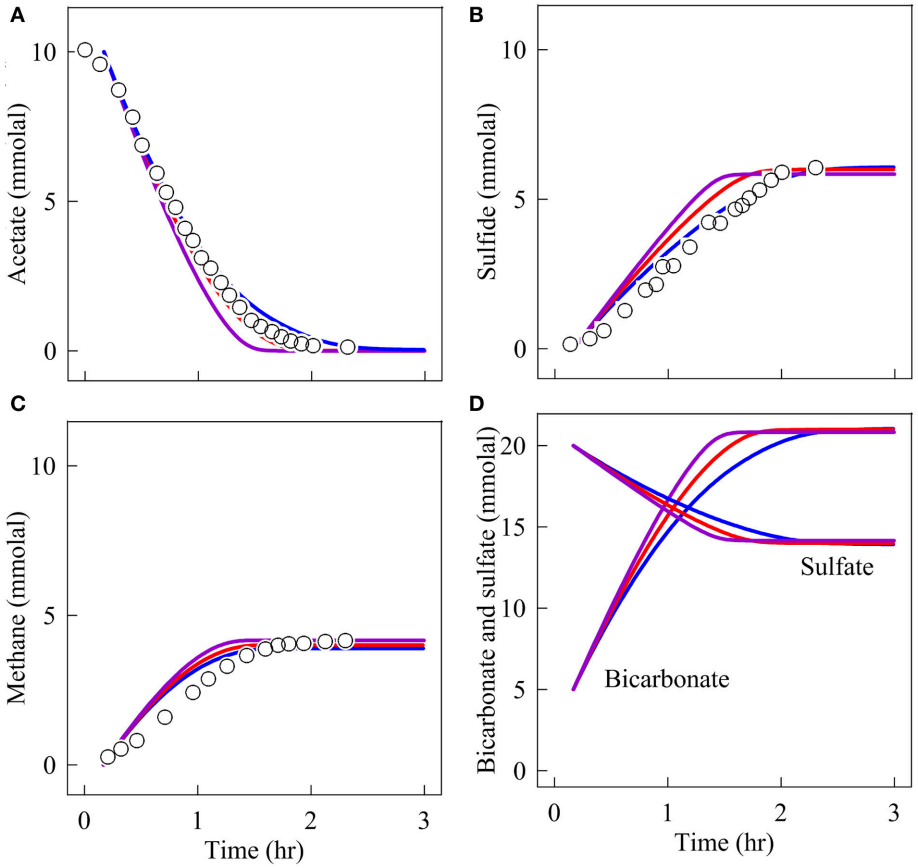

FIGURE 1 | Variation with time in the concentrations of acetate **(A)**, sulfide **(B)**, methane **(C)**, bicarbonate, and sulfate **(D)** in a batch reactor inoculated with *Desulfobacter postgatei* and *Methanosarcina barkeri*. Data points are the experimental results of Schönheit et al. (1982, their figure 3) at pH 7; the lines are the simulation results at pH 7 (blue), 6 (red), and 5 (purple) using microbial rate laws (Equations 3 and 10) and the parameters in **Table 1**.

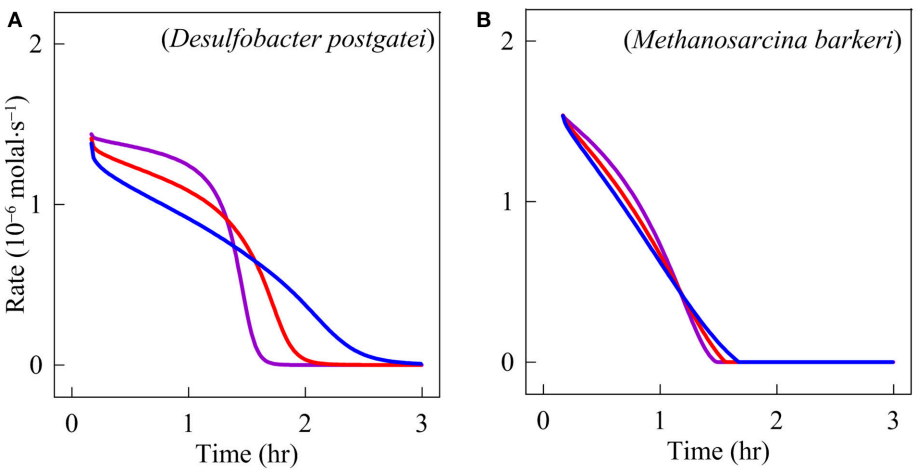

FIGURE 2 | Variation with time in respiration rates of *Desulfobacter postgatei* **(A)** and *Methanosarcina barkeri* **(B)**. The lines are the simulation results at pH 7 (blue), 6 (red), and 5 (purple).

addition to the thermodynamic control, methanogenesis rate is also limited by the concentration of acetate (Equation 3, **Figures 2B**, **3F**). Compared to *D. postgatei*, *M. barkeri* is more sensitive to the decrease in acetate concentrations because it has a relatively large half-saturation constant (**Table 1**). At pH 6 and 5, acetate concentration decreases faster than at pH 7, decreasing

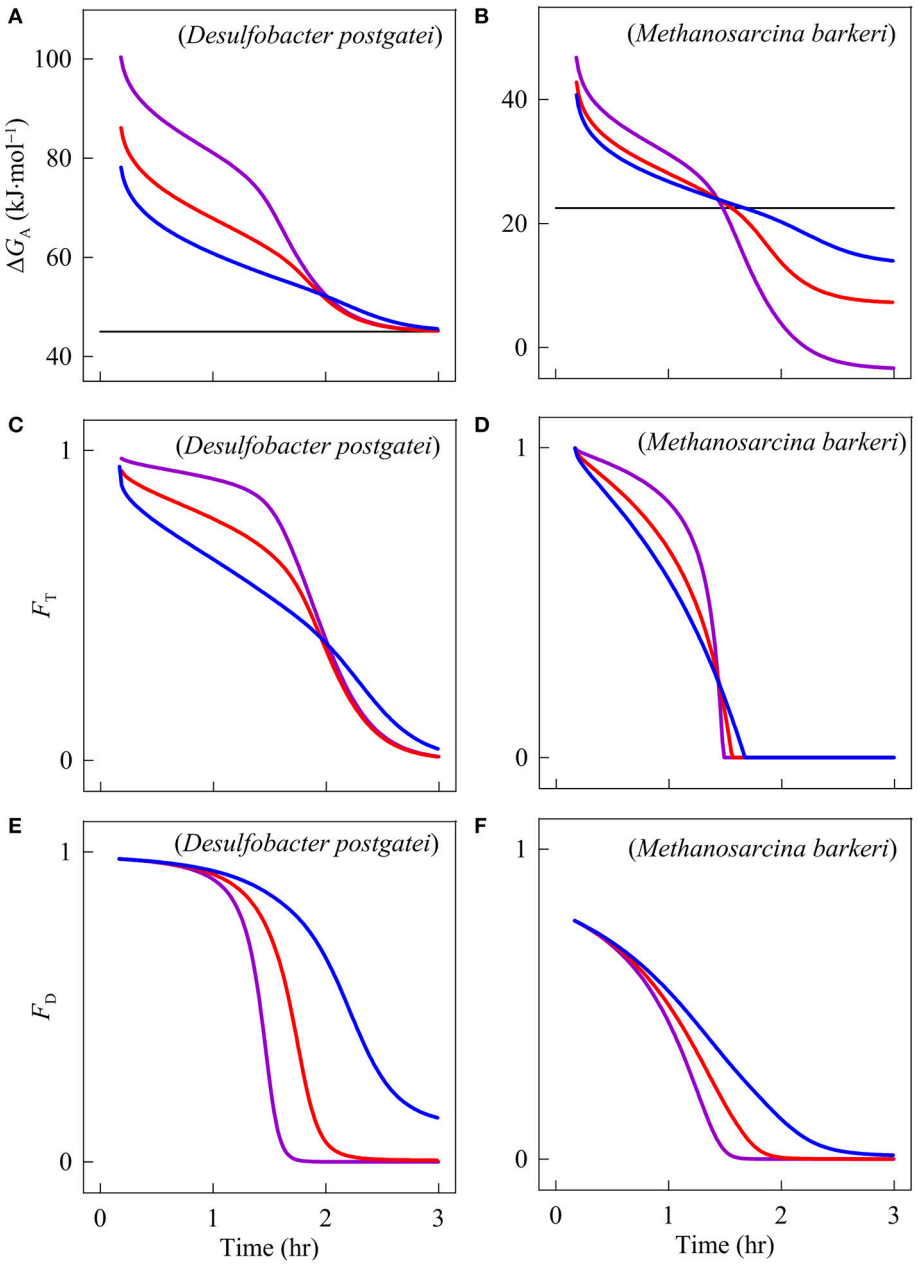

FIGURE 3 | Variation with time in the available energy ΔG_A **(A,B)**, the thermodynamic potential factor F_T **(C,D)**, and the kinetic factor F_D of *Desulfobacter postgatei* and *Methanosarcina barkeri* **(E,F)**. The lines are the simulation results at pH 7 (blue), 6 (red), and 5 (purple).

further the kinetic factor F_D of acetate (**Figures 1A**, **3F**). This change offsets the gain in energy provided by the decreasing pH and thus, the simulation predicts that the methanogenesis rate remains roughly unchanged at the different pHs.

Semi-open Environment

We then simulate the competition between *D. postgatei* and *M. barkeri* in a hypothetical semi-open system. We assume that fluid containing 5 mM acetate, 5 mM sulfate, and 1 mM bicarbonate has a temperature of 25°C and flows continuously through the system with a residence time of 3.7 day (or a turnover rate of 0.27 per day). We carry out the simulation at different pHs, from 5 to 7, for 10 years, well pass the time (0.5 year) when the system reaches steady state.

Figure 4 shows the simulation results. At pH 7, *D. postgatei* dominates the system but fails to drive out *M. barkeri*. At steady state, the hypothetical system contains 4.56 mM sulfide, 0.46 sulfide, 0.25 mM methane, and 0.21 mM acetate. *D. postgatei* grows to a concentration of 0.54 $g \cdot kg^{-1}$, and consumes 94.8% of the acetate flowing into the system. In contrast, *M. barkeri* has a

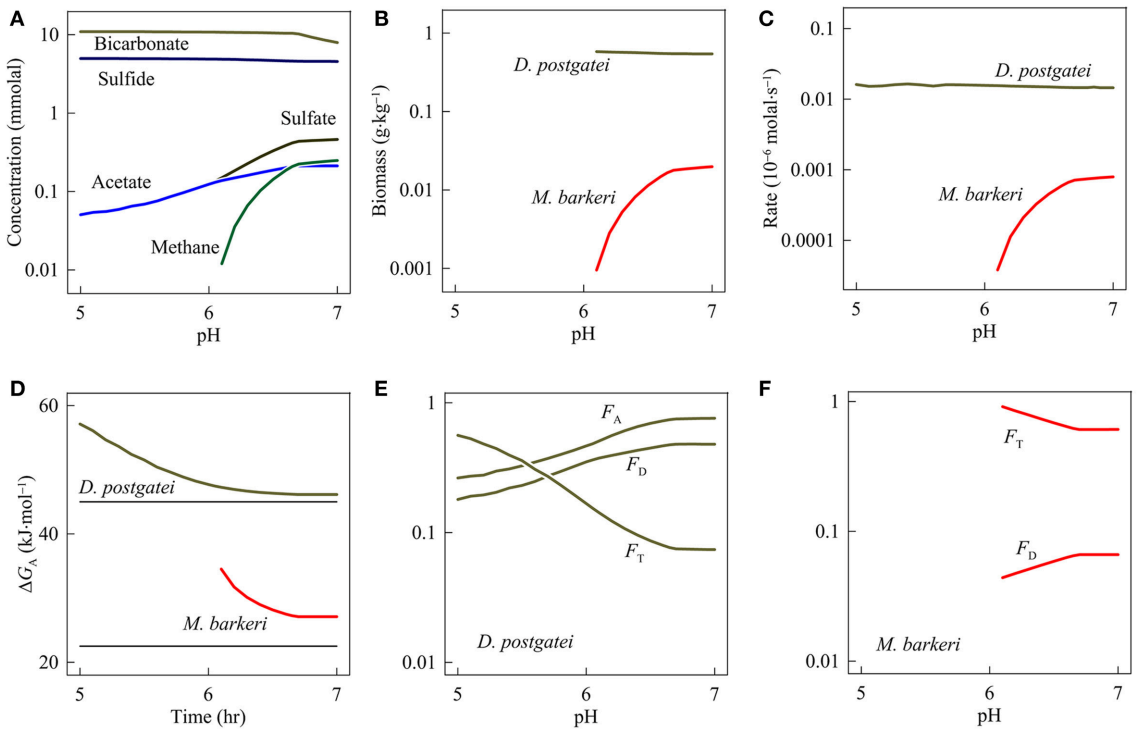

FIGURE 4 | Variation with pH in the concentrations of bicarbonate, sulfide, sulfate, acetate, and methane **(A)**, and the biomass concentrations **(B)**, the respiration rates **(C)**, the available energies ΔG_A **(D)**, the thermodynamic potential factors F_T, and the kinetic factors F_D and F_A of *Desulfobacter postgatei* **(E)** and *Methanosarcina barkeri* **(F)**.

concentration of 0.02 g·kg^{-1} and consumes the remaining 5.2% of the acetate.

As pH decreases from 7 to 6.1, *M. barkeri* persists but decreases in abundance relative to *D. postgatei*. Sulfate, acetate, and methane concentrations fall to 0.15, 0.14, and 0.01 mM, respectively, at pH 6.1 while sulfide concentration rises to 4.87 mM. Coupled with these changes, *D. postgatei* biomass rises slightly to 0.58 g·kg^{-1} as pH decreases to 6.1 while *M. barkeri* biomass decreases to 0.95 mg·kg^{-1}. At this point, methanogenesis only accounts for about 0.2% of the acetate consumption.

Only at pH equal to or less than 6, can *D. postgatei* drive *M. barkeri* out of the system. At pH 5, sulfate and acetate concentrations both decrease to 0.05 mM. The concentrations of sulfide and *D. postgatei* biomass rise to 4.97 mM and 0.59 g·kg^{-1}, respectively.

Above pH 6, the failure of *D. postgatei* to exclude *M. barkeri* is due to the significant thermodynamic limitation on sulfate reduction (**Figure 4D**). This control reflects the combined effects of neutral to near-neutral pH, acetate consumption, and bicarbonate and sulfide accumulation. As a consequence, the thermodynamic potential factor remains relatively small, lowering the rates of sulfate reduction and biosynthesis (Equations 3 and 10). To maintain biosynthesis rates above the rate of maintenance and cell death and thereby to avoid a decline in the biomass concentration, *D. postgatei* must balance the small thermodynamic potential factor by maintaining a modest kinetic factor of acetate. Specifically, it must maintain acetate concentrations above 0.13 mM, obtaining a kinetic factor above 0.4 (**Figure 4F**). In turn, these acetate concentrations are large enough for *M. barkeri* to achieve biosynthesis rates above the rate of maintenance and cell death (**Table 1**) and to survive in the system.

On the other hand, between pH 5 and 6, the energy available to *D. postgatei* rises well above the conserved energy (**Figure 4D**), raising the thermodynamic potential factor above 0.2. Under this condition, *D. postgatei* can lower acetate concentrations below the levels required for the survival of *M. barkeri*. These results are consistent with the hypothesis that sulfate reducers can drive methanogens out of the system by holding acetate concentrations below the levels needed for sustaining methanogen populations (Bethke et al., 2008). The results also support our hypothesis that pH can control the membership and metabolic activity of microbial consortia, and influence the outcome of microbial competition.

Syntrophy

A classic example of syntrophy is the interspecies hydrogen transfer, which takes place between H_2-producing and H_2-consuming microbes (Schink and Stams, 2013). Previous studies have emphasized H_2 levels as a determining factor of H_2-based syntrophic interactions. For example, butyrate-oxidizing microbes, such as *Syntrophomonas wolfei*, can oxidize butyrate to acetate by reducing protons to H_2. For butyrate oxidation

to remain thermodynamically favorable, butyrate oxidizers can partner with microbes that consume H_2 and thereby maintain H_2 levels low. In the companion paper (Jin and Kirk, 2018), we show that pH can play a similar role as H_2– pH affects the thermodynamics of both butyrate oxidation and hydrogentrophic redox reactions. Therefore, we expect that pH can also affect the kinetics of individual redox reactions in the syntrophic interaction and the dynamics of syntrophic consortia.

Laboratory Experiments

Wu et al. (1994) studied butyrate degradation using a consortium of three microbes, butyrate-oxidizing strain IB, *Methanobacterium formicium*, and *Methanosarcina mazei*. In their experiments, strain IB oxidizes butyrate and produces acetate and H_2,

$$\text{Butyrate} + 2H_2O \rightleftarrows 2\text{Acetate} + 2H_2 + H^+ \quad (13)$$

M. formicium catalyzes hydrogenotrophic methanogenesis,

$$4H_2 + H^+ + HCO_3^- \rightleftarrows CH_4 + 3H_2O \quad (14)$$

M. mazei drives acetoclastic methanogenesis (reaction 12). The three microbes grew at 37°C in batch reactors of 108 mL headspace and 50 mL growth medium. The medium had a pH of 7 and contained 4.3 mM butyrate, 4.1 mM isobutyate, 6.3 mM acetate, and 48.0 mM bicarbonate.

Jin (2007) developed a kinetic model for the three microbes. This model computes microbial reaction rates according to (Equations 3 and 10), and simulates butyrate degradation by accounting for the response of syntrophic energy conservation to H_2 partial pressure (Equation 8). Here we update the microbial parameters of the model to reflect recent developments of biogeochemical reaction modeling (see **Table 1**), and repeat the simulation.

According to the experimental observations and the simulation results at pH 7 (**Figure 5**), butyrate and isobutyrate concentrations decrease with time and are nearly depleted after day 25. Acetate concentration remains relatively stable during the first 10 days of the experiments and then accumulates to 10 mM after day 20. H_2 partial pressure peaks during the first couple of days and then decreases to 10^{-4} atm and remains at this level till day 20. Afterwards, H_2 partial pressure decreases to about 4.0×10^{-5} atm at day 27. The simulation also predicts the accumulations of dissolved inorganic carbon (DIC) and methane. At day 27, DIC reaches 57 mM and methane has a partial pressure of 0.17 atm.

Figure 6 shows the variations with time in the biomass concentrations and respiration rates of strain IB, *M. mazei*, and *M. formicium* according to the simulation results. The biomass concentrations of the three microbes vary similarly over time. They first increase to maximum values over about 20 days and then start to decrease slowly. Around day 20, the consortium is dominated by *M. mazeri*, whose maximum biomass concentration is 38.1 $mg{\cdot}kg^{-1}$. The biomass concentrations of strain IB and *M. formicium* are only 5.2 and 9.5 $mg{\cdot}kg^{-1}$, respectively. The rates of butyrate oxidation and hydrogenotrophic methanogenesis also vary similarly. The rates increase during the first 19 days, and then drop to 0. In comparison, the rate of *M. mazei* peaks twice during the experiments. The first peak appears around day 12 and the second comes on day 19, the same time when strain IB and *M. formicium* reach their maximum rates of butyrate oxidation and hydrogenotrophic methanogenesis, respectively.

Similar patterns of rates and biomass concentrations of strain IB and *M. formicium* confirm that the metabolisms of the two microbes depend on each other and thus interact syntrophically. On the other hand, the rate variation of *M. mazei* suggests that its metabolism is not closely coupled to butyrate oxidation, likely because acetate was provided at the beginning of the experiments.

pH Impact

To explore how pH may potentially affect butyrate degradation by the microbial consortium, we re-ran the updated model with medium at pH 6 and at pH 5. The results suggest that lowering pH can influence microbial metabolisms and interactions in at least three ways.

First, a decrease in pH affects butyrate degradation rates and hence the carbon fluxes from butyrate to CO_2 and methane. The simulation results indicate that, relative to pH 7, butyrate consumption slows by 4 and 15 days, respectively, at pH 6 and 5 (**Figure 5A**). Accordingly, lowering pH also delays variations in the biomass concentration and the respiration rate of strain IB (**Figures 6A,D**). For example, at pH 7, the biomass concentration reaches its maximum value at day 20. At pH 6 and 5, the maximum values appear on day 26 and 39, respectively. This delay in the metabolism explains the absence of an initial H_2 peak at pH 6 and 5 (**Figure 5E**).

The delay in butyrate degradation can be accounted for by the thermodynamic response of syntrophic butyrate oxidation. For strain IB, both the available energy and conserved energy depend on the partial pressures of H_2. At pH 7, the available energy first decreases briefly because of the H_2 peak and then increases to more than 10 $kJ{\cdot}mol^{-1}$ after day 5 (**Figure 7A**). Conserved energy also drops at the beginning of the experiments and then recovers, exceeding 5 $kJ{\cdot}mol^{-1}$ after day 5 (**Figure 7B**). As a result, the thermodynamic drive declines initially and then rises to about 7 $kJ{\cdot}mol^{-1}$ after day 5 (**Figure 7C**). The drive remains at this level until day 15 and then starts to decrease because of acetate accumulation. After day 20, the drive decreases to nearly 0.

Available energy also depends on pH. Specifically, available energy decreases with decreasing pH (Jin and Kirk, 2018). Thus, the thermodynamic drive is smaller at pH 6 than pH 7. At pH 5, during the first 10 days, the available energy is relatively large because of the small H_2 partial pressure. But the small partial pressure also allows strain IB to save more energy. As a result, the thermodynamic drive remains smaller than the value at pH 6. Smaller thermodynamic drives at pH 6 and 5 slow down the metabolism of strain IB (**Figure 7F**).

The delay in butyrate oxidation affects the metabolisms of *M. formicium* and *M. mazei*. *M. formicium* depends on strain IB for the supply of H_2. As a result, the delayed butyrate oxidation also delays the metabolism of *M. formicium*. The acetate for *M. mazei* comes from two sources, the acetate provided at the beginning of the experiments and the acetate produced by strain IB. The two different sources give rise to the two

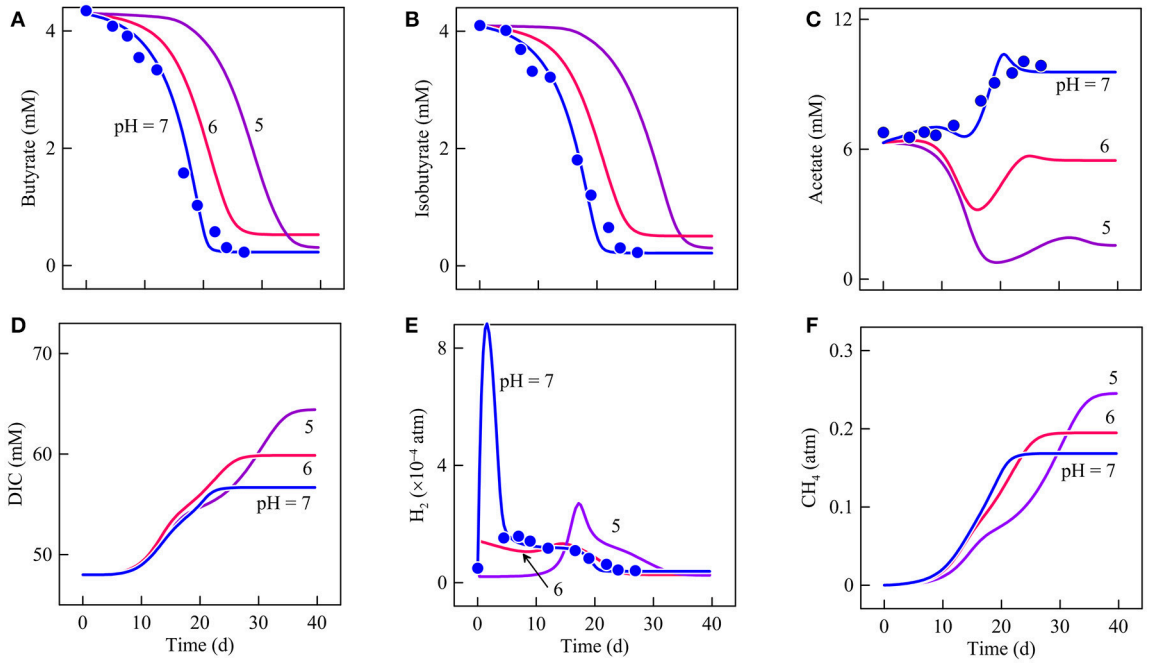

FIGURE 5 | Variation with time in the concentrations of butyrate **(A)**, isobutyrate **(B)**, acetate **(C)**, dissolved inorganic carbon (DIC, **D**), and the partial pressures of H_2 **(E)** and methane **(F)** in batch reactors of differ pHs. Data points are the results of Wu et al. (1994); lines are the results of biogeochemical reaction modeling, accounting for the impact of pH on the energy available from microbial reactions.

peak rates (**Figure 6E**). The first peak is made possible by the consumption of the initial acetate supply and the second is due to the acetate produced by butyrate oxidation. Delayed butyrate oxidation, therefore, delays the arrival of the second peak.

Second, a decrease in pH may also modulate the interactions between hydrogenotrophic and acetoclastic methanogenesis. In the reactors, methanogenesis by *M. mazei* is inhibited by the accumulation of methane. Methane accumulation decreases the thermodynamic drives and hence rates of both *M. formicium* and *M. mazei* (**Figures 7D,E,G,H**). But *M. mazei* is affected more because the energy available from acetoclastic methanogenesis (reaction 12) tends to be smaller than that of hydrogenotrophic methanogenesis (reaction 14), and because *M. mazei* conserves more energy than *M. formicium* per methane (Equations 6 and 7, **Table 1**). These thermodynamic differences allow *M. formicium* to make a proportionally larger contribution to methane production than *M. mazei.*

This effect can be evaluated in terms of the contribution of *M. mazei* to methane production. In the reactors, 4.3 mM butyrate, 4.1 mM isobutyrate and 6.3 mM acetate are provided. If the metabolisms of *M. mazei* and *M. formicium* are independent of each other and are not inhibited by methane accumulation, *M. formicium* would produce 4.2 mol methane, and *M. mazei* would produce 23.1 mol per liter of medium. In other words, *M. mazei* would account for 84.6% of methane production. According to the simulation results, at pH 7, *M. mazei* accounts for 76.1% of methane production. Thus, methane accumulation decreases the contribution of *M. mazei* by 8.5%.

At lower pH, this effect is lessened because methane production by *M. formicium* is delayed. The delay gives *M. mazei* an opportunity to consume more acetate and to make a bigger contribution to methane production (**Figures 5C,F, 6B,E**). At pH 6 and 5, *M. mazei* accounts for 80.9 and 83.9% of methane production, respectively. Corresponding to the increasing methane production, the biomass concentration of *M. mazeri* also increases (**Figures 6B,C**). At pH 6, *M. mazeri* reaches a maximum biomass concentration of 45.8 $mg{\cdot}kg^{-1}$ at day 28. At pH 5, the maximum biomass concentration of 57.4 $mg{\cdot}kg^{-1}$ is achieved on day 58.

Lastly, the pH decreases may regulate the efficiency of methane production. Microbial communities degrade organic carbon to CO_2 and methane. The efficiency of methane production is quantified as the ratio of methane production to the sum of CO_2 and methane productions (Ye et al., 2012),

$$\eta = \frac{C_{CH_4}}{C_{CO_2} + C_{CH_4}}, \tag{15}$$

where C_{CO_2} and C_{CH_4} are the total CO_2 and methane produced in the reactors. In the experiments, methane is produced by both acetoclastic and hydrogenotrophic methanogenesis but CO_2 is produced only by acetoclastic methanogenesis. The hydrogenotrophic pathway instead consumes CO_2. As such, the efficiency of methane generation increases with the increasing contribution of hydrogenotrophic methanogenesis. According to the simulation results, the proportion of acetoclastic to hydrogenotrophic methanogenesis changes with pH. Therefore,

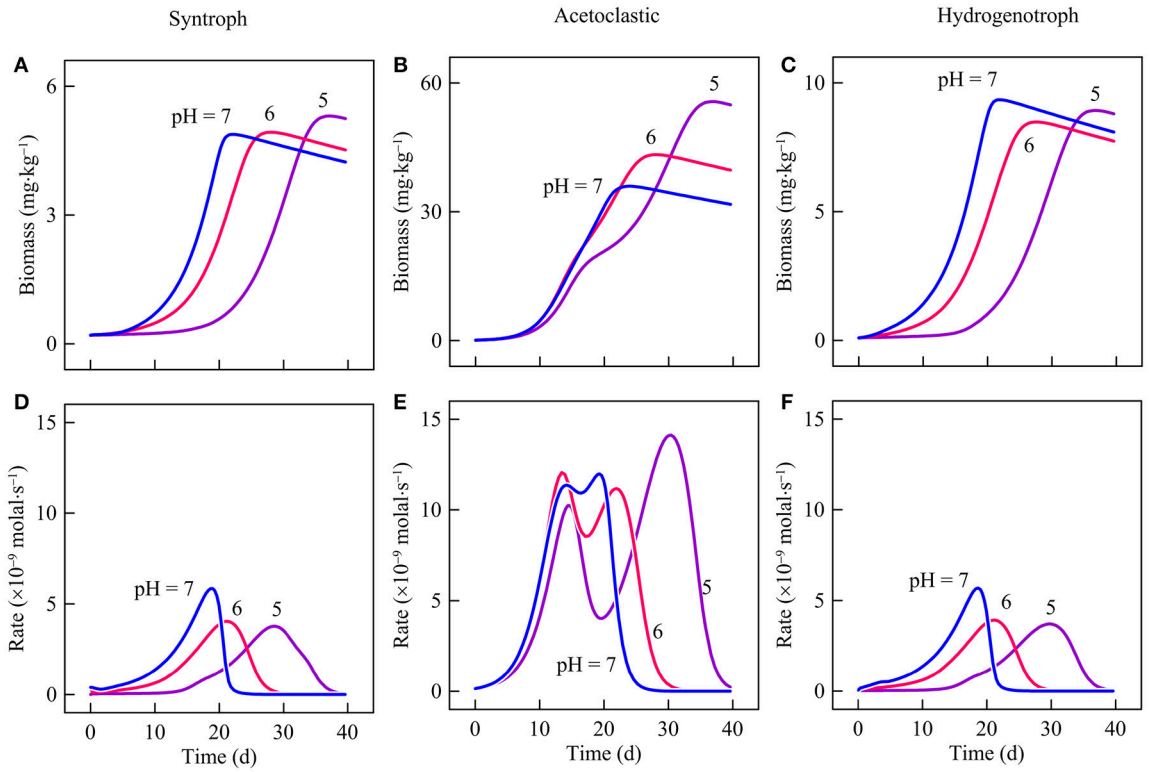

FIGURE 6 | Variation with time in the biomass concentrations and respiration rates of strain IB **(A,D)**, *Methanosarcina mazei* **(B,E)**, and *Methanobacterium formicium* **(C,F)** in batch reactors of differ pHs. Lines are the results of biogeochemical reaction modeling, accounting for the impact of pH on the energy available from microbial reactions.

the methane production efficiency η also varies with pH. Specifically, a decrease in pH lowers the efficiency of methane production. According to the simulation results, at pH 7, the efficiency of methane production is 65.7%. At pH 6 and 5, the efficiency decreases to 61.8 and 59.6%, respectively.

DISCUSSION

We explored the relationship between pH and microbial communities using biogeochemical kinetic modeling. We simulated how pH variation speeds up or slows down microbial respiration and growth and in turn influences microbial interactions, including the competition between sulfate reducers and methanogens and the syntrophy among butyrate oxidizers and methanogens.

Kinetic Response

In the companion paper (Jin and Kirk, 2018), we show that the variations in environmental pH change significantly the energy yields of syntrophic oxidation, sulfate reduction, and methanogenesis. In this paper, we simulate the kinetics of these processes using the thermodynamically consistent Monod equation (Equation 6)—this equation accounts for the energy yields of microbial redox reactions as well as the energy conserved by respiration. The simulation results show that a decrease in pH speeds up the metabolism of acetotrophic sulfate reducers. Specifically, decreases of one pH unit speed up the progress by 12%. The decrease in pH also slows down the metabolism of butyrate syntrophic oxidizers. A decrease of one pH unit decreases the rate by >10%. These results are consistent with the predictions from the thermodynamics of the redox reactions (reactions 11 and 13), and support that the thermodynamic responses of redox reactions can be strong enough to affect the kinetics of microbial metabolisms.

The pH decreases also raise the energy yields of acetoclastic and hydrogenotrophic methanogenesis (reactions 12 and 14) and hence have the potential of raising the metabolic activities of methanogens (Jin and Kirk, 2018). But our kinetic simulations fail to support these predictions. The inconsistencies between the thermodynamic and kinetic predictions highlight the complexity of microbial kinetics and the importance of microbial interactions.

For example, the rate of acetoclastic methanogenesis depends on the kinetic factor of acetate concentration as well as the thermodynamic factor of the energy yield. The modeling results show that in the batch reactor experiments of Schönheit et al. (1982), the pH decreases do raise the energy yields of acetoclastic methanogenesis, but this increasing effect is counteracted by the decreasing acetate concentrations. As a result, the rate doesn't respond much to the pH changes (**Figures 1–3**).

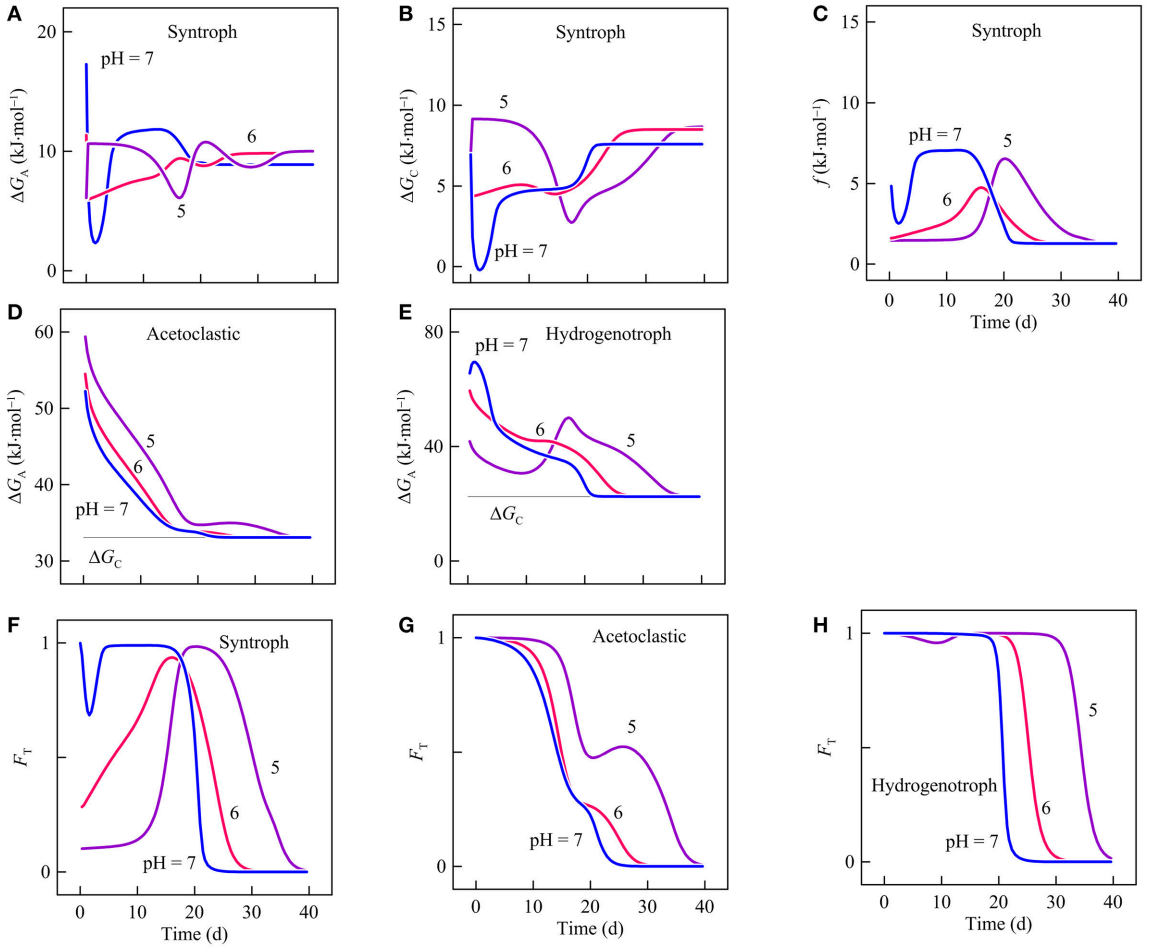

FIGURE 7 | Variation with time in the energy available **(A)**, the conserved energy **(B)**, and the thermodynamic drive **(C)** of strain IB, the energy available to *Methanosarcina mazei* **(D)** and to *Methanobacterium formicium* **(E)**, and the thermodynamic factor of syntrophic butyrate oxidation **(F)**, acetoclastic methanogenesis **(G)**, and hydrogenotrophic methanogenesis **(H)** in batch reactors of differ pHs. Lines are the results of biogeochemical reaction modeling, accounting for the impact of pH on the energy available from microbial reactions.

In the experiments of Wu et al. (1994), the pH decreases do not raise the energy yield of hydrogenotrophic methanogenesis. In the experiments, H_2-consuming *M. formicium* relies on H_2-producing strain IB for the supply of H_2. The energy yield of hydrogenotrophic methanogenesis depends not only on pH but also on the concentrations of H_2. At lower pH, H_2 production from butyrate oxidation slows down and H_2 concentration decreases, thereby lowering the energy yield at the beginning of the experiments and slowing down hydrogenotrophic methanogenesis.

The discrepancies between the thermodynamic predictions and kinetic modeling reiterate the difference between thermodynamic and kinetic modeling: the predictions made from reaction thermodynamics should be treated as the potential responses of microbial metabolisms. Whether the predictions are relevant or not requires biogeochemical modeling that considers not only the kinetics of microbial metabolisms of interest, but also the impact from concurrent biogeochemical processes.

Competitive Exclusion vs. Co-occurrence

In addition to the observation-based modeling, we also simulated the competition between *D. postgatei* and *M. barkeri* in a hypothetical semi-open environment (**Figure 4**). The results show that, despite its kinetic and thermodynamic advantages, *D. postgatei* is not always capable of excluding *M. barkeri* from the system, and that environmental pH can play a role in the outcome of microbial competition. The simulation demonstrates that pH can determine whether competitors coexist or are excluded from the environment. These results might help resolve the disagreement between the principle of competitive exclusion and metabolic diversities in natural environments.

According to the principle of competitive exclusion (Hardin, 1960), where different microbes reduce various electron acceptors by competing for a limiting electron donor, they cannot coexist, and only the one with competitive advantage can survive. In natural sediments and aquifers, common electron acceptors include O_2, nitrate, ferric minerals, sulfate, and CO_2,

and the apparent pattern in electron acceptor usage appears to conform to this principle (Kuivila et al., 1989; Chapelle et al., 1995; Bethke et al., 2011). Among these electron acceptors, O_2 is the most thermodynamically favorable one, followed by nitrate, ferric mineral, sulfate, and CO_2, respectively. Accordingly, O_2 is typically the first electron acceptor to be depleted from the environment, whereas CO_2 is the last.

But different anaerobic respiration reactions can take place simultaneously. The co-occurrence of iron reduction, sulfate reduction, and methanogenesis have been discovered in various settings, from biofilms to surface sediments and aquifers (Raskin et al., 1996; Metje and Frenzel, 2007; Flynn et al., 2013). Different mechanisms have been proposed to account for these co-occurrences, including spatial heterogeneity, dynamic biogeochemical conditions, and complex microbial interactions (Roy and Chattopadhyay, 2007; Bethke et al., 2011).

In our modeling example (**Figure 4**), *D. postgatei* can consume acetate and grow faster than *M. barkeri* (**Table 1**). But under the assumed flow and chemical conditions, the competitive exclusion principle only applies at pH $\leq$ 6.0. At pH above 6.0, the two microbes co-exist, due to the relatively significant thermodynamic limitation on the rates of sulfate reduction and biosynthesis. To balance the thermodynamic limitation, *D. postgatei* must maintain acetate at relatively large concentrations in order to achieve a relatively large kinetic factor F_D of acetate. These acetate concentrations exceed thresholds required for sustaining *M. barkeri* population.

Between pH 5 and 6, the relatively low pH raises the energy yield of sulfate reduction, which loosens the thermodynamic control and raises the rates of sulfate reduction and biosynthesis. Such favorable thermodynamic response allows *D. postgatei* to exclude *M. barkeri* by lowering acetate concentrations.

These results suggest that the competitive exclusion principle may not always be applicable, especially where microbes of competitive advantage are subject to significant thermodynamic limitations. They also illustrate a decisive role of pH in the outcome of microbial competition, and support our hypothesis that environmental pH is capable of shaping microbial community composition by affecting the thermodynamics and kinetics of individual microbial metabolisms.

Microbial Kinetic Model

This study focuses on how microbial thermodynamic responses to pH may affect the kinetics of individual microbial metabolism and the outcome of microbial interactions. In addition, pH also directly affects the catalytic capacity of microbes, therefore the kinetic parameters of microbial respiration and growth (Equation 3). This impact arises from the dependence of enzyme activities on cytoplasmic pH. Cytoplasmic pH modifies enzyme conformations and is critical for the formation and maintenance of the catalytically-competent active sites within enzymes (Leprince and Quiquampoix, 1996; Nielsen and McCammon, 2003). In addition, many enzymes are regulated allosterically by effector molecules. The presence of effector molecules and their interactions with enzymes depend on cytoplasmic pH (Makhlynets et al., 2015). Although cytoplasmic pH is tightly regulated by microbes, it does vary in accordance with the changes in environmental pH, albeit to lesser extents (Booth, 1985; Kobayashi et al., 2000; Padan et al., 2005).

Current models consider the direct pH impact on the forward rates by including a pH factor (Ng and Schaffner, 1997; Tienungoon et al., 2000). Enzyme activities respond to pH variations by following bell- or triangular-shaped curve. For example, the pH impact can be described using a triangular function,

$$F_{\mathrm{pH}} = \begin{cases} \frac{\mathrm{pH_{opt}} - \mathrm{pH}}{\mathrm{pH_{opt}} - \mathrm{pH_{min}}}, & \mathrm{pH_{min}} \leq \mathrm{pH} \leq \mathrm{pH_{opt}}; \\ \frac{\mathrm{pH_{max}} - \mathrm{pH}}{\mathrm{pH_{max}} - \mathrm{pH_{opt}}}, & \mathrm{pH_{opt}} < \mathrm{pH} \leq \mathrm{pH_{max}}. \end{cases} \quad (16)$$

Here pH_{opt}, pH_{min}, and pH_{max} are the optimal, minimum, and maximum pHs for growth. We propose to determine the values of pH_{opt}, pH_{min}, and pH_{max} based on the pH response of rate-limiting enzymes of microbial respiration. For example, methyl-coenzyme reductase is likely a rate-limiting step of methanogenesis (Bonacker et al., 1992). Based on previous laboratory observations of methyl-coenzyme M reductase of *Methanosarcina thermophila* (Jablonski and Ferry, 1991), we set pH_{opt} at 6.9, pH_{min} at 4.9, and pH_{max} at 8.9.

By combining the pH factor and the thermodynamic factor, we consider not only the direct impact of pH on respiration enzymes, but also the indirect impact by changing the thermodynamics of microbial respiration. These dual effects may explain a common pattern in the response of microbial metabolism to pH—the metabolic response is asymmetric about optimal pH. Specifically, between the minimum and optimal pHs, the slope of the increase in microbial rates differs from the slope of decrease between optimal and maximum pHs. The asymmetric responses have been widely reported for laboratory cultures, including syntrophs (Zhang et al., 2005; Hatamoto et al., 2007), iron reducers (Xu et al., 2005; Sun et al., 2014), sulfate reducers (Baena et al., 1998; O'Flaherty et al., 1998), and methanogens (Zehnder and Wuhrmann, 1977; Huser et al., 1982).

Taking acetoclastic methanogenesis as an example, according to the pH factor (Equation 16), a deviation from optimal pH always leads to the inhibition of microbial metabolism. Likewise, moving pH toward optimal pHs would promote microbial metabolism. However, for neutrophilic methanogens whose optimal pH is 7, increases in pH above the optimal pH raise their thermodynamic drives and hence rates, counteracting decreases by the direct pH effect on the forward rates of methanogenesis.

Combining the pH factor and the thermodynamic factor, the modified Monod equation predicts that rates of acetoclastic methanogenesis respond to pH asymmetrically. As shown in **Figure 8**, the slope predicted for the rate increase between pH_{min} and pH_{opt} is almost twice as large as the slope predicted for the decrease between pH_{opt} and pH_{max}. This prediction agrees with previous laboratory observations, such as those of *Methanosarcina mazei* (Maestrojuan and Boone, 1991).

In simulating microbial metabolisms, we purposely set the pH factor to one (Equation 16). In other words, we assumed that pH only impacts the thermodynamics of microbial redox reactions. This assumption allows us to focus on microbial thermodynamic responses. Despite this simplification, the simulation may still be relevant to natural environments, especially those that host

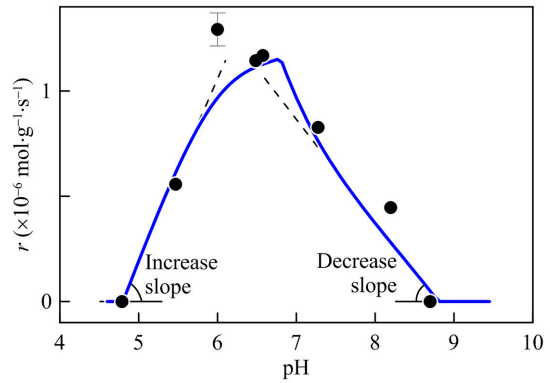

FIGURE 8 | Variation with time in the rate of acetoclastic methanogenesis. Solid line is the prediction by the pH factor and the thermodynamic factor, assuming that acetate is abundant and the kinetic factor F_D takes a value of one; data points are computed from the experimental results of *Methanosarcina mazei*, using a growth yield of 2 g·(mol acetate)$^{-1}$ (Maestrojuan and Boone, 1991). The slopes of increase and decrease are 0.86 and 0.49 mol·g^{-1}·s^{-1} per pH unit, respectively.

diverse microbial communities. For example, environments with neutral pH may host a seed bank of microbes whose optimal pHs are at pH 6 or 5. Thus, lowering pH to 6 lowers the respiration rate for microbes with optimal pH of 7, but would raise the rate for those with optimal pH of 6 (or their pH factors become one). As a result, microbes with an optimal pH of 6 would take over and drive out those whose optimal pHs are not 6, providing that other microbial properties, such as growth yields and maintenance rates, do not change.

Consistent with this interpretation, results of Petrie et al. (2003) and Kirk et al. (2013) suggest that the contribution of *Anaeromyxobacter* species to iron reduction increased as pH decreased in their field and bioreactor studies, respectively. As shown in the companion paper, iron reduction becomes more thermodynamically favorable as pH decreases. Thus, the shift in iron reducer identity was not likely a response to a thermodynamic limitation but possibly a reflection of differences in pH optima. These observations suggest that our results are best applied to environments that host diverse communities of microorganisms with different optimal pHs. We further propose that thermodynamics may provide insight into the kinetic response of microbial metabolisms to pH variations, whereas pH optima may dictate the identity of species that catalyze the reactions at a given pH.

Concluding Comments

We applied biogeochemical kinetic modeling to simulate the responses of syntrophic butyrate oxidation, sulfate reduction, and methanogenesis to pH changes. Our modeling is biased by two assumptions. We assume that pH does not affect the amount of energy conserved by microbes. We also assume that microbial kinetic parameters, including rate constants, half-saturation constants, and maintenance rates, do not change with pH. These assumptions overlook the complexity of microbial metabolisms and may have underestimated the extent to which pH impacts cell metabolisms. But these assumptions allow us to focus on microbial thermodynamic responses and to test whether the pH-induced thermodynamic responses alone are strong enough for significant changes in the composition and activity of microbial communities.

The simulation results show that, by accounting for the thermodynamics and kinetics of microbial reactions and the interactions among microbes, biogeochemical kinetic modeling can be applied to gauge and tune the predictions made from thermodynamics. For example, a pH decrease from 7 to 6 or to 5 raises the energy yield of acetotrophic sulfate reduction, but lowers the energy yield of syntrophic butyrate oxidation. Based on the thermodynamic responses, we predict that acetotrophic sulfate reduction would speed up, but syntrophic butyrate oxidation would slow down by the pH decrease. The kinetic modeling results confirm the predictions—a one-unit decrease in pH can raise the rate of acetotrophic sulfate reduction and lower the rate of syntrophic butyrate oxidation by >10%.

Our results also show that thermodynamic predictions are not always relevant. A pH decrease from 7 to 6 or to 5 raises the energy yield of acetoclastic and hydrogenotrophic methanogenesis, and hence can speed up the two reactions. But the kinetic modeling results suggest that, in closed environments, such as in laboratory batch reactors, the thermodynamic influence of pH on acetoclastic methanogenesis can be canceled by the impact of decreasing acetate concentrations. Also, where hydrogenotrophic methanogens live syntrophically with H_2-producing butyrate oxidizers, both the energy yield and rate of methanogenesis may depend primarily on the H_2 production by butyrate oxidizers, instead of environmental pH.

The simulation of the semi-open system supports the hypothesis that by changing the energy yields of microbial redox reactions, environmental pH is capable of changing the composition of microbial communities. According to the simulation results, environmental pH dictates the outcome of the competition between *D. postgatei* and *M. barkeri*. Between pH 6 and 7, despite the competitive advantage of *D. postgatei* over *M. barkeri*, the two microbes live together in the system. Between pH 5 and 6, only *D. postgatei* stays, and *M. barkeri* disappears. The different outcomes come from the influence of pH on the energy yield of sulfate reduction. Between pH 6 and 7, *D. postgatei* is subject to a significant thermodynamic limitation, and must balance that limitation by keeping acetate concentrations relatively large—large enough for sustaining the cells of *M. barkeri*. Decreasing pH to or below 6 alleviates the thermodynamic limitation and enables *D. postgatei* to expel *M. barkeri* by lowering acetate concentrations below the minimum levels required for sustaining *M. barkeri*.

By raising or lowering the energy yields of microbial redox reactions, environmental pH is also capable of shaping the ecological functions of microbial communities. The modeling results of butyrate syntrophic degradation show that pH variation is capable of changing microbially-driven carbon fluxes in three ways. First, environmental pH affects the magnitudes of carbon fluxes. Lowering pH from 7 to 5 decrease the rates of butyrate oxidation and hence the fluxes of C from butyrate to CO_2 and

methane. This decrease is mainly due to the decreases in the energy available from the syntrophic oxidation of butyrate.

Second, environmental pH regulates the contributions of hydrogenotrophic and acetoclastic methanogenesis to methane production. Compared to the hydrogenotrophic pathway, acetoclastic methanogenesis is more sensitive to the accumulation of methane in the environment because of its limited available energy. The simulation results show that lowering pH from 7 to 5 decreases the thermodynamic drive of the hydrogenotrophic pathway and subsequently its production of methane. In turn, this effect alleviates the methane inhibition of the acetoclastic pathway, allowing it to produce more methane.

Last, variation in pH changes the efficiency of methane production. By working together, syntrophic butyrate oxidation, and hydrogenotrophic and acetoclastic methanogenesis convert butyrate to CO_2 and methane. Environmental pH can influence the efficiency of methane production by changing the relative significances of the two methanogenesis pathways. Specifically, decreases in pH decrease the efficiency of methane production from butyrate, a result that is consistent with previous observations in wetlands (Ye et al., 2012). Taken together, these results provide a mechanistic view of how environmental pH modulate the fluxes and composition of C in the environment. Although we focused on butyrate degradation, we expect that pH also influence the C fluxes from other organic compounds and hence the biogeochemical cycling of C—a topic to be further investigated.

In addition, the modeling results add to the current theories of environmental microbiology. For example, current theories attribute microbial competitive advantages to two different mechanisms—by lowering substrate levels below the thresholds required for driving the catabolisms of competitors (Lovley et al., 1982) or below the thresholds for sustaining the populations of competitors (Bethke et al., 2008). Our simulation results suggest that the two mechanisms are applicable to two different environmental settings—the first is applicable to batch reactors and other closed environments, whereas the second applies to flow-through reactors or other semi-open environments.

The modeling results also suggest that the principle of competitive exclusion may not always be applicable. This principle predicts that where electron donors are limiting, microbial respiration reactions segregated into spatially-distinct zones. According to the simulation results, this principle may not be applicable to respiration reactions of significant thermodynamic limitations, where the energy yields of redox reactions are close to the energy conserved by respiration. Under this condition, respiration reactions of competitive advantage may take place simultaneously with reactions of competitive disadvantage. Only where the thermodynamic control becomes relatively insignificant, can the respiration reactions of competitive advantage exclude competing reactions from the environment by lowering electron donor concentrations. Thus, by modifying the energy yields of microbial redox reactions, environmental pH can determine whether the competitive exclusion principle is applicable, or whether different microbial redox reactions take place simultaneously or segregated into different zones.

AUTHOR CONTRIBUTIONS

All authors listed have made a substantial, direct and intellectual contribution to the work, and approved it for publication.

FUNDING

This research was funded by the National Science Foundation under Award EAR-1636815 and by National Aeronautics and Space Administration under Grant NNX16AJ59G.

SUPPLEMENTARY MATERIAL

The Supplementary Material for this article can be found online at: https://www.frontiersin.org/articles/10.3389/fenvs.2018.00101/full#supplementary-material

REFERENCES

Amenabar, M. J., Shock, E. L., Roden, E. E., Peters, J. W., and Boyd, E. S. (2017). Microbial substrate preference dictated by energy demand rather than supply: *Nat. Geosci*. 10, 577–581. doi: 10.1038/ngeo2978

Baena, S., Fardeau, M. L., Labat, M., Ollivier, B., Garcia, J. L., and Patel, B. K. C. (1998). *Desulfovibrio aminophilus* sp. nov., a novel amino acid degrading and sulfate reducing bacterium from an anaerobic dairy wastewater lagoon. *Syst. Appl. Microbiol*. 21, 498–504. doi: 10.1016/S0723-2020(98)80061-1

Bethke, C. M. (2008). *Geochemical and Biogeochemical Reaction Modeling.* Cambridge:Cambridge University Press.

Bethke, C. M., Ding, D., Jin, Q., and Sanford, R. A. (2008). Origin of microbiological zoning in groundwater flows. *Geology* 36, 739–742. doi: 10.1130/G24859A.1

Bethke, C. M., Sanford, R. A., Kirk, M. F., Jin, Q., and Flynn, T. M. (2011). The thermodynamic ladder in geomicrobiology. *Am. J. Sci*. 311, 183–210. doi: 10.2475/03.2011.01

Bonacker, L. G., Baudner, S., and Thauer, R. K. (1992). Differential expression of the two methyl-coenzyme M reductases in *Methanobacterium thermoautotrophicum* as determined immunochemically via isoenzyme-specific antisera. *Eur. J. Biochem.* 206, 87–92. doi: 10.1111/j.1432-1033.1992.tb16904.x

Booth, I. R. (1985). Regulation of cytoplasmic pH in bacteria. *Microbiol. Rev*. 49, 359–378.

Chapelle, F. H., McMahon, P. B., Dubrovsky, N. M., Fujii, R. F., Oaksford, E. T., and Vroblesky, D. A. (1995). Deducing the distribution of terminal electron-accepting processes in hydrologically diverse groundwater systems. *Water Resour. Res*. 31, 359–371. doi: 10.1029/94WR02525

Delany, J. M., and Lundeen, S. R. (1990). *The LLNL Thermodynamical Database.* Lawrence Livermore National Laboratory Report UCRL-21658.

Flynn, T. M., Sanford, R. A., Ryu, H., Bethke, C. M., Levine, A. D., Ashbolt, N. J., et al. (2013). Functional microbial diversity explains groundwater chemistry in a pristine aquifer. *BMC Microbiol.* 13:146. doi: 10.1186/1471-2180--146

Hardin, G. (1960). The competitive exclusion principle. *Science* 131, 1292–1297. doi: 10.1126/science.131.3409.1292

Hatamoto, M., Imachi, H., Fukayo, S., Ohashi, A., and Harada, H. (2007). *Syntrophomonas palmitatica* sp. nov., an anaerobic, syntrophic, long-chain

fatty-acid-oxidizing bacterium isolated from methanogenic sludge. *Int. J. Syst. Evolu. Microbiol.* 57, 2137–2142. doi: 10.1099/ijs.0.64981-0

Helgeson, H. C. (1969). Thermodynamics of hydrothermal systems at elevated temperatures and pressures. *Am. J. Sci.* 267, 729–804. doi: 10.2475/ajs.267.7.729

Huser, B. A., Wuhrmann, K., and Zehnder, A. J. B. (1982). *Methanothrix soehngenii* gen. nov. sp. nov., a new acetotrophic non-hydrogen-oxidizing methane bacterium. *Arch. Microbiol.* 132, 1–9.

Jablonski, P. E., and Ferry, J. G. (1991). Purification and properties of methyl coenzyme M methylreductase from acetate-grown *Methanosarcina thermophila*. *J. Bacteriol.* 173, 2481–2487. doi: 10.1128/jb.173.8.2481-2487.1991

Jin, Q. (2007). Control of hydrogen partial pressures on the rates of syntrophic microbial metabolisms: a kinetic model for butyrate fermentation. *Geobiology* 5, 35–48. doi: 10.1111/j.1472-4669.2006.00090.x

Jin, Q. (2012). Energy conservation of anaerobic respiration. *Am. J. Sci.* 312, 573–628. doi: 10.2475/06.2012.01

Jin, Q., and Bethke, C. M. (2002). Kinetics of electron transfer through the respiratory chain. *Biophys. J.* 83, 1797–1808. doi: 10.1016/S0006-3495(02)73945-3

Jin, Q., and Bethke, C. M. (2003). A new rate law describing microbial respiration. *Appl. Environ. Microbiol.* 69, 2340–2348. doi: 10.1128/AEM.69.4.2340-2348.2003

Jin, Q., and Bethke, C. M. (2005). Predicting the rate of microbial respiration in geochemical environments. *Geochim. Cosmochim. Acta* 69, 1133–1143. doi: 10.1016/j.gca.2004.08.010

Jin, Q., and Bethke, C. M. (2007). The thermodynamics and kinetics of microbial metabolism. *Am. J. Sci.* 307, 643–677. doi: 10.2475/04.2007.01

Jin, Q., and Kirk, M. F. (2016). Thermodynamic and kinetic response of microbial reactions to high CO2. *Front. Microbiol.* 7:1696. doi: 10.3389/fmicb.2016.01696

Jin, Q., and Kirk, M. F. (2018). pH as a primary control in environmental microbiology: 1. Thermodynamic perspective. *Front. Environ. Sci.* 6:21. doi: 10.3389/fenvs.2018.00021

Jin, Q., and Roden, E. E. (2011). Microbial physiology-based model of ethanol metabolism in subsurface sediments. *J. Contam. Hydrol.* 125, 1–12. doi: 10.1016/j.jconhyd.2011.04.002

Jin, Q., Roden, E. E., and Giska, J. R. (2013). Geomicrobial kinetics: extrapolating laboratory studies to natural environments. *Geomicrobiol. J.* 30, 173–185. doi: 10.1080/01490451.2011.653084

Kinniburgh, D. G., van Riemsdijk, W. H., Koopal, L. K., Borkovec, M., Benedetti, M. F., and Avena, M. J. (1999). Ion binding to natural organic matter: competition, heterogeneity, stoichiometry and thermodynamic consistency. *Colloids Surf. A Physicochem. Eng. Aspects* 151, 147–166. doi: 10.1016/S0927-7757(98)00637-2

Kirk, M. F., Santillan, E. F. U., Sanford, R. A., and Altman, S. J. (2013). CO2-induced shift in microbial activity affects carbon trapping and water quality in anoxic bioreactors. *Geochim. Cosmochim. Acta* 122, 198–208. doi: 10.1016/j.gca.2013.08.018

Kobayashi, H., Saito, H., and Kakegawa, T. (2000). Bacterial strategies to inhabit acidic environments. *J. Gen. Appl. Microbiol.* 46, 235–243. doi: 10.2323/jgam.46.235

Konings, W. N., Albers, S.-V., Koning, S., and Driessen, A. J. M. (2002). The cell membrane plays a crucial role in survival of bacteria and archaea in extreme environments. *Antonie van Leeuwenhoek* 81, 61–72. doi: 10.1023/A:1020573408652

Kotsyurbenko, O. R., Chin, K.-J., Glagolev, M. V., Stubner, S., Simankova, M. V., Nozhevnikova, A. N., et al. (2004). Acetoclastic and hydrogenotrophic methane production and methanogenic populations in an acidic West-Siberian peat bog. *Environ. Microbiol.* 6, 1159–1173. doi: 10.1111/j.1462-2920.2004.00634.x

Kuivila, K. M., Murray, J. W., Devol, A. H., and Novelli, P. C. (1989). Methane production, sulfate reduction and competition for substrates in the sediments of Lake Washington. *Geochim. Cosmochim. Acta* 53, 409–416. doi: 10.1016/0016-7037(89)90392-X

Leprince, F., and Quiquampoix, H. (1996). Extracellular enzyme activity in soil: effect of pH and ionic strength on the interaction with montmorillonite of two acid phosphatases secreted by the ectomycorrhizal fungus *Hebeloma cylindrosporum*. *Eur. J. Soil Sc.* 47, 511–522. doi: 10.1111/j.1365-2389.1996.tb01851.x

Lovley, D. R., Dwyer, D. F., and Klug, M. J. (1982). Kinetic analysis of competition between sulfate reducers and methanogens for hydrogen in sediments. *Appl. Environ. Microbiol.* 43, 1373–1379.

Lovley, D. R., and Klug, M.J. (1982). Intermediary metabolism of organic matter in the sediments of a eutrophic lake. *Appl. Environ. Microbiol.* 43, 552–560.

Lovley, D. R., and Philips, E. J. (1987). Competitive mechanisms of sulfate reduction and methane production in the zone of ferric iron reduction in sediments. *Appl. Environ. Microbiol.* 53, 2636–2641.

Maestrojuan, G. M., and Boone, D. R. (1991). Characterization of Methanosarcina barkeri MST and 227, *Methanosarcina mazei* S-6T, and *Methanosarcina vacuolata* Z-761T. *Int. J. Syst. Evolu. Microbiol.* 41, 267–274. doi: 10.1099/00207713-41-2-267

Makhlynets, O. V., Raymond, E. A., and Korendovych, I. V. (2015). Design of allosterically regulated protein catalysts. *Biochemistry* 54, 1444–1456. doi: 10.1021/bi5015248

Metje, M., and Frenzel, P. (2007). Methanogenesis and methanogenic pathways in a peat from subarctic permafrost. *Environ. Microbiol.* 9, 954–964. doi: 10.1111/j.1462-2920.2006.01217.x

Molongoski, J. J., and Klug, M. J. (1980). Anaerobic metabolism of particulate organic matter in the sediments of hypereutrophic lake. *Freshw. Biol.* 10, 507–518. doi: 10.1111/j.1365-2427.1980.tb01225.x

Monokova, S.V. (1975). Volatile fatty acids in bottom sediments of the Rybinsk reservoir. *Hydrobiol. J.* 11, 45–48.

Ng, T. M., and Schaffner, D. W. (1997). Mathematical models for the effects of pH, temperature, and sodium chloride on the growth of *Bacillus stearothermophilus* in salty carrots. *Appl. Environ. Microbiol.* 63, 1237–1243.

Nielsen, J. E., and McCammon, J. A. (2003). Calculating pKa values in enzyme active sites. *Protein Sci.* 12, 1894–1901. doi: 10.1110/ps.03114903

Nielsen, U. N., Ayres, E., Wall, D. H., and Bardgett, R. D. (2011). Soil biodiversity and carbon cycling: a review and synthesis of studies examining diversity–function relationships. *Eur. J. Soil Sci.* 62, 105–116. doi: 10.1111/j.1365-2389.2010.01314.x

O'Flaherty, V., Mahony, T., O'Kennedy, R., and Colleran, E. (1998). Effect of pH on growth kinetics and sulphide toxicity thresholds of a range of methanogenic, syntrophic and sulphate-reducing bacteria. *Process Biochem.* 33, 555–569. doi: 10.1016/S0032-9592(98)00018-1

Padan, E., Bibi, E., Ito, M., and Krulwich, T. A. (2005). Alkaline pH homeostasis in bacteria: new insights. *Biochim. Biophys. Acta Biomembranes* 1717, 67–88. doi: 10.1016/j.bbamem.2005.09.010

Panikov, N. S. (1995). *Microbial Growth Kinetics.* London: Chapman and Hall.

Paul, A., Stösser, R., Zehl, A., Zwirnmann, E., Vogt, R. D., and Steinberg, C. E. W. (2006). Nature and abundance of organic radicals in natural organic matter: effect of pH and irradiation. *Environ. Sci. Technol.* 40, 5897–5903. doi: 10.1021/es060742d

Petrie, L., North, N. N., Dollhopf, S. L., Balkwill, D. L., and Kostka, J. E. (2003). Enumeration and characterization of iron(III)-reducing microbial communities from acidic subsurface sediments contaminated with uranium(VI). *Appl. Environ. Microbiol.* 69, 7467–7479. doi: 10.1128/AEM.69.12.7467-7479.2003

Raskin, L., Rittmann, B. E., and Stahl, D. A. (1996). Competition and coexistence of sulfate-reducing and methanogenic populations in anaerobic biofilms: *Appl. Environ. Microbiol.* 62, 3847–57.

Rosso, L., Lobry, J. R., Bajard, S., and Flandrois, J. P. (1995). Convenient model to describe the combined effects of temperature and pH on microbial growth. *Appl. Environ. Microbiol.* 61, 610–616.

Roy, S., and Chattopadhyay, J. (2007). Towards a resolution of 'the paradox of the plankton': a brief overview of the proposed mechanisms. *Ecol. Complex* 4, 26–33. doi: 10.1016/j.ecocom.2007.02.016

Schink, B., and Stams, A. J. M. (2013). "Syntrophism among prokaryotes," in *The Prokaryotes: Prokaryotic Communities and Ecophysiology,* eds E. Rosenberg, E. F. DeLong, S. Lory, E. Stackebrandt, and F. Thompson (Berlin; Heidelberg: Springer), 471–493.

Schönheit, P., Kristjansson, J. K., and Thauer, R. K. (1982). Kinetic mechanism for the ability of sulfate reducers to out-compete methanogens for acetate. *Arch. Microbiol.* 132, 285–288.

Sun, D., Wang, A., Cheng, S., Yates, M., and Logan, B. E. (2014). *Geobacter anodireducens* sp. nov., an exoelectrogenic microbe in bioelectrochemical systems. *Int. J. Syst. Evolu. Microbiol.* 64, 3485–3491. doi: 10.1099/ijs.0.061598-0

Thauer, R. K., Jungermann, K., and Decker, K. (1977). Energy conservation in chemotrophic anaerobic bacteria. *Bacteriolog. Rev*. 41, 100–180.

Thompson, L. R., Sanders, J. G., McDonald, D., Amir, A., Ladau, J., Locey, K. J., et al. (2017). A communal catalogue reveals Earth's multiscale microbial diversity. *Nature* 551, 457–463. doi: 10.1038/nature24621

Tienungoon, S., Ratkowsky, D. A., McMeekin, T. A., and Ross, T. (2000). Growth limits of *Listeria monocytogenesas* a function of temperature, pH, NaCl, and lactic acid. *Appl. Environ. Microbiol*. 66, 4979–4987. doi: 10.1128/AEM.66.11.4979-4987.2000

van Bodegom, P. (2007). Microbial maintenance: a critical review on its quantification. *Microbiol Ecol*. 53, 513–523. doi: 10.1007/s00248-006-9049-5

Wu, W.-M., Jain, M. K., and Zeikus, J. G. (1994). Anaerobic degradation of normal- and branched-chain fatty acids with four or more carbons to methane by a syntrophic methanogenic triculture. *Appl. Environ. Microbiol*. 60, 2220–2226.

Xavier, J. B. (2011). Social interaction in synthetic and natural microbial communities. *Mol. Syst. Biol*. 7:483. doi: 10.1038/msb.2011.16

Xu, M., Guo, J., Cen, Y., Zhong, X., Cao, W., and Sun, G. (2005). *Shewanella decolorationis* sp. nov., a dye-decolorizing bacterium isolated from activated sludge of a waste-water treatment plant. *Int. J. Syst. Evolu. Microbiol*. 55, 363–368. doi: 10.1099/ijs.0.63157-0

Ye, R., Jin, Q., Bohannan, B., Keller, J. K., McAllister, S. A., and Bridgham, S. D. (2012). pH controls over anaerobic carbon mineralization, the efficiency of methane production, and methanogenic pathways in peatlands across an ombrotrophic–minerotrophic gradient. *Soil Biol. Biochem*. 54, 36–47. doi: 10.1016/j.soilbio.2012.05.015

Zehnder, A. J. B., and Wuhrmann, K. (1977). Physiology of a *Methanobacterium* strain AZ. *Arch. Microbiol*. 111, 199–205. doi: 10.1007/BF00549357

Zhang, C., Liu, X., and Dong, X. (2005). *Syntrophomonas erecta* sp. nov., a novel anaerobe that syntrophically degrades short-chain fatty acids. *Int. J. Syst. Evol. Microbiol*. 55, 799–803. doi: 10.1099/ijs.0.63372-0

Conflict of Interest Statement: The authors declare that the research was conducted in the absence of any commercial or financial relationships that could be construed as a potential conflict of interest.